Proceedings of the 2006 American Control Conference
Minneapolis, Minnesota, USA, June 14-16, 2006

Predicting instabilities in gas-lifted wells simulation

Laure Sinègre*, Nicolas Petit
Centre Automatique et Systèmes
École des Mines de Paris
60, Bd Saint-Michel, 75272 PARIS Cedex
Email: sinegre,petit@cas.ensmp.fr
*corresponding author

Philippe Ménégatti
Centre Scientifique et Technique Jean Féger
TOTAL
Avenue Larribeau, 64000 PAU
Email: philippe.menegatti@total.com

Abstract— **In this paper we study two classes of instabilities occurring in practical applications of gas-lifted oil wells. The model underlying our analysis stresses the role of the feedback interconnection. It involves an infinite dimensional linear system coupled to a first order dynamics. Stability analysis is performed through the small gain theorem and the relevance of the derived conclusions is discussed in terms of state of some of state of the art well production knowledge.**

I. INTRODUCTION

Producing oil from deep reservoirs and lifting it through wells to surface facilities often requires activation to maintain oil output at a commercial level. In the gas-lift activation technique [4], gas is injected at the bottom of the well through the injection valve (point C in Figure 1) to lighten up the fluid column and to lower the gravity pressure losses. High pressure gas is injected at well head through the gas valve (point A), then goes down into the annular space between the drilling pipe (casing, point B) and the production pipe (tubing, point D) where it enters. Oil produced from the reservoir (point F) and injected gas mix in the tubing. They flow through the production valve (point E) located at the surface.

As wells and reservoirs get older, liquid rates begin to decrease letting wells be more sensitive to flow instabilities commonly called headings. These induce important oil production losses (see [12]) along with possible facilities damages. While the consequence of these instabilities have been referenced for long time (see [8] for example), the involved mechanisms are rarely explained.

The best identified instability is the "casing-heading". It consists of a succession of pressure build-up phases in the casing without production and high flow rate phases due to intermittent gas injection rate from the casing to the tubing (see [14] or [21] for a complete description). General stability criteria have been proposed. Unlike [22], these various approaches do not rely on steady state equations. In [2], the key assumption is that stability is guaranteed if an increase of downhole tubing pressure causes a drop of mixture density and if the gas conduit depletes faster than the tubing pressure. Then, differential equations are used to derive criterion taking the form of a set of inequalities. A more dynamical system oriented approach can be found in [3]. The analysis relies on Routh's criterion and a detailed study of the root locations of a third order transfer function when physical parameters of interest vary. In [1], a unified criteria based on previous studies of [3] and [2] is proposed. In all these works the oil column is considered homogenous, which implicitly neglects the propagation phenomenon in the tubing. These models are mainly devoted to the study of casing-heading for which this simplifying assumption is particularly valid. Yet, another mechanism have been brought to light by [12]: the density-wave. Even though the gas injection rate through valve C is kept constant, self-sustained oscillations, confined in the tubing D can occur. Out-of-phase effects between the well influx and the total pressure drop along the tubing are usually reported at the birth of this phenomenon.

The contribution of this paper is the study and analysis of gas lifted wells as the feedback connection of a distributed parameter system (to take into account the propagation in the tubing) and a stable first order (the casing as a buffer tank). This approach aims at encompassing both casing-heading and density-wave phenomena. Existence of complex behaviors due to attractive limit cycle induced by saturations (as detailed in [18]) is studied through the analysis of a linearized model around an equilibrium point. This defines stability criteria. A partial differential equation model of the tubing dynamics is presented. A delay system rewriting is derived under the form of an integral equation. The reservoir is treated as a boundary condition. The connection of casing and tubing subsystems is achieved through the injection valve, which is modelled with a saturation function. This seemingly cascaded system contains feedback loops at two different levels. The first loop appears in the tubing itself through the gravity terms in Bernoulli's law. The second loop takes place by means of the state dependant connecting term (injection valve) which serves as an input for the propagation equation. Stability of each subsystem is characterized. Additionally, input output gain are computed and the small gain theorem allows us to conclude towards stability of the whole system when the asymptotic condition of large amount of injected gas holds. This analysis is in accordance to experimental observations. It stresses the contribution of each subsystem design parameters and operating points to the stability of the global system.

The paper is organized as follows. In Section II, we study the tubing subsystem and conclude on sufficient condition for stability. In particular, we detail the role of various

1-4244-0210-7/06/$20.00 ©2006 IEEE

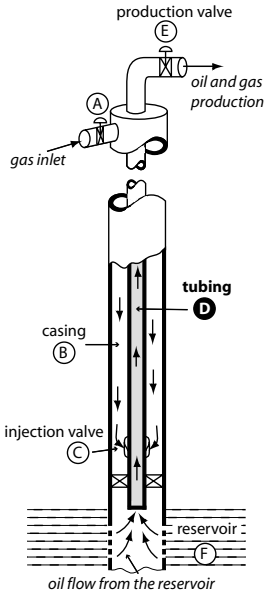

Fig. 1. Gas-lift activated well. Casing-heading involves both tubing D and casing B while density-wave takes place in the tubing D.

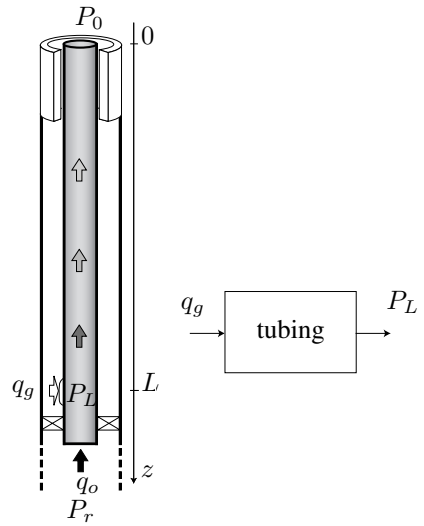

(a) Outline (b) Block scheme

Fig. 2. (a) Outline of the tubing. Oil from the reservoir and gas from the casing mix at $z = L$ resulting in a gas mass fraction that propagates up to the surface. (b) the tubing as a SISO collocated system which input is q_g, gas mass flow rate from the casing, and output is P_L, the downhole pressure.

parameters in our proposed model and show the consistency with some state of the art wells production knowledge. In Section III, we connect the casing dynamics to the tubing, and study the obtained interconnection's stability through the small gain theorem. We propose the interpretation of well-known phenomena at the light of our model. In conclusion the density-wave phenomenon is interpreted as the stability loss due to the internal tubing feedback loop. Besides, the casing-heading phenomenon arises from the interconnection of the two systems. Future directions are given in Section IV.

II. Tubing analysis

In this section, we focus on the propagation phenomenon in the tubing. We explicit an integral equation model, and, from its stability analysis, we discuss under which condition density-wave instability can occur. The tubing appears as a finite-memory delayed system which stability is guaranteed by applying the small-gain theorem to its inner feedback connection.

A. Density-wave instability description

The tubing can be considered as a 1D pipe filled with oil from the reservoir and gas fed by the casing (see Figure 2(a)). Nomenclature is given in Table I. From a system point of view, the tubing is a collocated SISO system with the gas mass flow rate, q_g, as input and the pressure at the bottom of the well, P_L, as output (see Figure 2(b)).

1) Simulation setup with OLGA®2000: Figure 3 shows an example of the so-called "density-wave instability" simulated with the transient multi-phase flow simulator OLGA®2000 [17] used with the compositional tracking and Matlab-OLGA link toolboxes. The tubing is divided into two branches (see Figure 4), linked by the `INJECTION` node: the `BOTTOM-HOLE` branch, a 100 m long vertical pipe lying below the injection point and the `TUBING` branch, a 2400 m long vertical pipe. The gas injection is modelled by a 350 m long horizontal pipe (`BUFFER`) connecting a source of gas to the `INJECTION` node through a downstream flow controlled valve. To each terminal node corresponds a boundary condition: at the `WELL-HEAD` a constant pressure condition and at both `OIL-INLET` and `GAS-INLET` a pressure/flow condition, i.e. oil reservoir `RES` and `GAS-SOURCE` respectively supply oil and gas flow rates proportionally to local pressure differences. The fluid characterization is limited to two components and heat transfert are neglected. Some of the constants used in the simulation are referenced in Table I and signalled by $^{(1)}$.

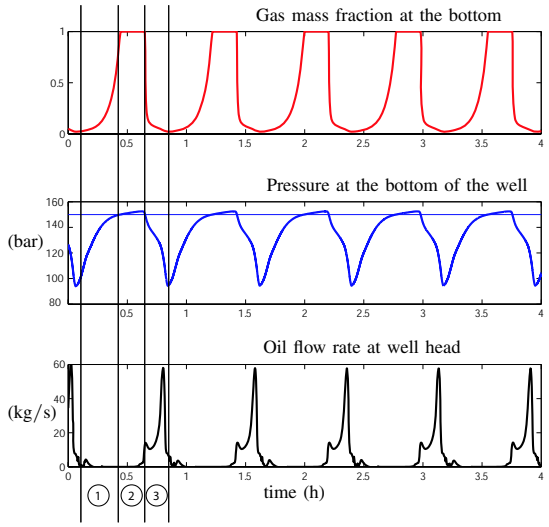

Fig. 3. Density wave simulated with OLGA®2000.

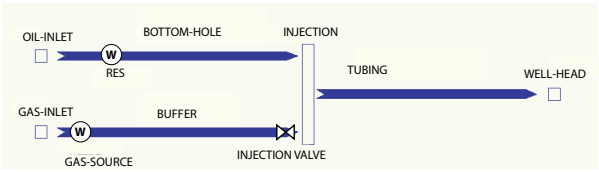

Fig. 4. Block scheme of the OLGA®2000 simulation setup for the density-wave study. Three pipes are considered along with two sources and one injection valve.

2) Density-wave phenomenon description: Typically, the depth of the well is 2500 m and the reservoir pressure is 150 bar. Oil production has an oscillating behavior consisting of 3 main phases.

1) There is no oil production at the surface but P_L, the pressure at the bottom of the well, is less than the reservoir pressure. Thus oil enters the pipe, letting P_L get closer to 150 bar. This is the self regulating mechanism of the well: the more is produced from the reservoir, the greater P_L becomes and eventually the less is produced. P_L is going to reach a constant which, in this case, is greater than 150 bar. The system switches to phase 2.
2) There is zero oil production at the surface and from the reservoir (saturation of the oil flow rate at the bottom of the well). The gas mass fraction, which is close to 0 in phase 1, gets to a strictly positive constant in phase 2. Finally, the oil produced from the reservoir in phase 1 reaches the surface and creates a pressure drop in the well.
3) P_L decreases below 150 bar, oil flow rate at the bottom of the well increases and brings the fall of the gas mass fraction.

In other words, the density wave can be summarized as the propagation of the mass fraction at the bottom of the well which is a result of a switching boundary condition.

B. Tubing model

1) Description and general assumptions: We represent the density wave instability as a monodimensional two phases flow problem. Mass conservation laws along with proper choice of slip velocity law (see [5] and [9]) yield a Riemann invariant (as defined in [6]), the gas mass fraction. The boundary condition is computed using Bernoulli's law. We assume that the gas is ideal and that no phase change occurs. Following [2], we neglect transient inflow from the reservoir as well as acceleration and friction terms in Bernoulli's law. In other words we assume the flow to be dominated by gravitational effects. Furthermore, for sake of simplicity, we approach the gas mass fraction by the gas volume fraction. The temperature of the well, the gas density gradient along the tubing, and the gas velocity are assumed constant.

Pressure law: Using Bernoulli's law we get

$$P(t,z) = P_0 + \int_0^z \rho_m(t,\zeta) g d\zeta \tag{1}$$

TABLE I
NOMENCLATURE †.

Symb.	Constants	Values	Units
R	Ideal gas constant	523	S.I.
T	Temperature of the well	303	K
C_{iv}	Injection valve constant		
S_a	Casing section	$0.0127^{(3)}$	m^2
α	Constant	$0.0304^{(3)}$	$1/m^3$
β	Constant	$4822^{(3)}$	$1/m/s^2$
PI	Productivity Index	$4e-6^{(1)}$	kg/s/Pa
		$2e-6^{(2)(3)}$	kg/s/Pa
P_r	Reservoir pressure	$150e5^{(1)(2a)(3)}$	Pa
		$180e5^{(2b)}$	Pa
		$220e5^{(2c)(3)}$	Pa
$P_L^\star$	Pres. of the column of oil	$P_0 + \rho_l g L$	Pa
P_0	Separator pressure	$10e5$	Pa
g	Gravity constant	9.81	m/s^2
ρ_l	Density of oil	781	kg/m^3
V^∞	Slip velocity constant	-	m/s
V_g	Gas velocity	0.8	m/s
κ	Threshold parameter	0.03	
L	Pipe length	2500	m
λ	Constant	$1/PI\,(1/\kappa - 1)$	1/(ms)

Symb.	Variables	Expressions	Units
$m_1(t)$	Mass of gas in the casing		kg
$P_a(t)$	Casing pressure		Pa
$\rho_a(t)$	Casing gas density		kg/m^3
$w_{gc}(t)$	Gas mass flow rate		kg/s
$V_L(t,z)$	Oil velocity	$V_g + V^\infty/R_l$	m/s
$Rg(t,z)$	Gas volume fraction		
$R_l(t,z)$	Oil volume fraction	$R_g + R_l = 1$	
$x(t,z)$	Gas mass fraction		
$P(t,z)$	Pressure of the well in the tubing		Pa
$x_L(t)$	Gas mass fraction at $z = L$		
$P_L(t)$	Pressure at $z = L$		Pa
$\rho_g(t,z)$	Gas density		ks/m^3
$\rho_m(t,z)$	Mixture density		ks/m^3
$q_o(t,z)$	Oil mass flux	$R_l \rho_l V_l$	$kg/s/m^2$
$q_g(t,z)$	Gas mass flux	$R_g \rho_g V_g$	$kg/s/m^2$

† Constant values used for the density-wave simulation (see section II-A.1) are signalled by $^{(1)}$. When used for the casing-heading simulation (see section III-A) the parameters are pointed out by $^{(3)}$. Values signalled by $^{(2)}$ are used for the simulation of section II-B.5. a, b and c correspond to $P_r = 150$, 180 and 220 bar respectively.

Density of the mixture is given by $1/\rho_m = x/\rho_g + (1-x)/\rho_l$. To work with a linear expression of ρ_m, we assume that

$$\rho_m \sim x\rho_g + (1-x)\rho_l \tag{2}$$

Equivalently, we assume that the gas mass density is close to the gas volume density, which is a valid assumption in practice. Further, in the derivation of the gas density, gas is considered ideal and temperature T constant. Besides we assume that the pressure gradient $\frac{P_r - P_0}{L}$ along the tubing is also constant, computed from boundary conditions. Simulations have shown that this simplification improves the tractability while saving the oscillatory behavior. Using expressions (2) for substitution in (1), we get

$$P(t,z) = P_0 + \rho_l g z + \int_0^z x(t,\zeta) g \left(\frac{(L-\zeta)P_0 + \zeta P_r}{LRT} - \rho_l \right) d\zeta \tag{3}$$

Slip velocity and Riemann invariant: We define the slip velocity as follows

$$V_g - V_l = \frac{V_\infty}{R_l}$$

Mass conservation laws write

$$\frac{\partial \rho_g R_g}{\partial t} + \frac{\partial w_{iv}}{\partial z} = 0 \tag{4}$$

$$\frac{\partial \rho_l R_l}{\partial t} + \frac{\partial q_l}{\partial z} = 0 \tag{5}$$

By definition

$$x = \frac{R_g \rho_g}{R_g \rho_g + R_l \rho_l} \tag{6}$$

One can combine (4), (5) and (6), to obtain $\frac{\partial x}{\partial t} + V_g \frac{\partial x}{\partial z} = 0$. This shows that x is a Riemann invariant and implies

$$x(t,z) = x\left(t - \frac{L-z}{V_g}, L\right) = x_L\left(t - \frac{L-z}{V_g}\right)$$

For sake of simplicity V_g is assumed constant. Therefore, values of bottom well gas mass fraction x_L over a time interval $[t-\delta, t]$ defines the profile $[0, L] \ni z \mapsto x(t,z)$ at time t. Using this expression in (3), and noting that $P_L(t) = P(t, L)$, we find

$$P_L(t) = P_L^\star + \int_{t-\tau}^{t} k(t-\zeta) x_L(\zeta) d\zeta \tag{7}$$

with

$$\tau = L/V_g \tag{8}$$

$$P_L^\star = P_0 + \rho_l g L \tag{9}$$

and

$$[0,\tau] \ni t \mapsto k(t) \triangleq V_g g \left(\frac{tP_0 + (\tau - t)P_r}{\tau RT} - \rho_l\right) < 0 \tag{10}$$

Notice that k is a strictly decreasing affine function. For sake of simplicity, we shall write for now on

$$k(t) = (k_1 t + k_2)\mathbf{1}_{[0,\tau]} \tag{11}$$

Where $\mathbf{1}_{[0,\tau]}$ is zero over the entire real line except for the interval $[0,\tau]$ where it is equal to 1.

2) Boundary condition: Classically (see [4]), the oil rate q_o is given at the reservoir boundary by the Productivity Index (PI) through

$$q_o(t, L) = PI \max(P_r - P_L(t), 0) \tag{12}$$

By definition,

$$x_L(t) = \frac{1}{1 + PI/q_g \max(P_r - P_L(t), 0)} \tag{13}$$

We want to simplify this last expression in the case of large values for PI. On one hand, as $P_r - P_L$ begins to be positive, x_L goes to zero. Let κ denote a threshold parameter. In particular $x_L < \kappa$ is equivalent to $P_L < P_r - \frac{q_g}{PI}(1/\kappa - 1)$. We denote

$$\lambda \triangleq \frac{1}{PI}(1/\kappa - 1) \tag{14}$$

On the other hand, when $P_L > P_r$, $x_L = 1$. Therefore, we consider x_L as constant, equal to 1 when $P_L > P_r$ and equal to 0 when $P_L < P_r - \lambda q_g$. Under this assumption, the expression of x_L reduces to

$$x_L = h(X),\ X \triangleq 1 - \frac{P_r - P_L}{\lambda q_g} \tag{15}$$

with $h(\cdot) = \max(\min(1, \cdot), 0)$. Equation (15) is the definition we use instead of equation (13) from now on.

3) Summary: density-wave as a distributed delay model: We now gather equations (7) and (15), and consider an initial condition $[-\delta, 0] \ni t \mapsto \phi(t) \in \mathbb{R}$. The following model represents the density wave phenomenon by the evolution of the pressure at the bottom of the well P_L

$$\begin{cases} P_L(t) = P_L^\star + \displaystyle\int_0^\tau k(\zeta) h\left(1 - \frac{P_r - P_L(t-\zeta)}{\lambda q_g(t-\zeta)}\right) d\zeta \\ P_L(t) = \phi(t),\ t \in [-\tau, 0] \end{cases} \tag{16}$$

where τ is the transport delay defined in (8), λ is a constant given in (14), $P_L^\star$, given in (9), is the pressure at the bottom of the pipe when it is full of oil, and P_r is the pressure of the reservoir. k is a finite support affine function, given in (10) and (11). It depends on the considered fluids.

4) Equilibrium point and stability analysis: Given a constant input $\overline{q}_g$, the unsaturated equilibrium $\overline{P}_L$ can be computed through the integral equation (16).

$$\overline{P}_L = P_L^\star + \left(1 - \frac{P_r - \overline{P}_L}{\lambda q_g}\right) \int_0^\tau k(\zeta) d\zeta$$

yielding

$$\overline{P}_L = \frac{\lambda \overline{q}_g \left(P_L^\star + \int_0^\tau k(\zeta) d\zeta\right) - P_r \int_0^\tau k(\zeta) d\zeta}{\lambda \overline{q}_g - \int_0^\tau k(\zeta) d\zeta} \tag{17}$$

Linearization of the dynamics of (16) around the steady value of the input and state $(\overline{q}_g, \overline{P}_L)$ yields

$$\begin{aligned} \delta P_L(t) = & \frac{1}{\lambda \overline{q}_g} \int_0^\tau k(\zeta) \delta P_L(t-\zeta) d\zeta \\ & + \frac{P_r - \overline{P}_L}{\lambda \overline{q}_g^2} \int_0^\tau k(\zeta) \delta q_g(t-\zeta) d\zeta \end{aligned} \tag{18}$$

Denoting $\delta \tilde{P}_L$ and $\delta \tilde{q}_g$ the Laplace transforms of δP_L and δq_g respectively, one gets

$$\delta \tilde{P}_L(s) = G(s) \delta \tilde{q}_g(s) \tag{19}$$

with

$$G(s) = \frac{P_r - \overline{P}_L}{\lambda \overline{q}_g^2} \frac{\tilde{k}(s)}{1 - \frac{\tilde{k}(s)}{\lambda \overline{q}_g}}, \quad \tilde{k}(s) = \int_0^\tau k(\zeta) e^{-s\zeta} d\zeta \tag{20}$$

Through this rewriting, the linearized dynamics of the tubing appears as a positive feedback connection (see Figure 5) which stands for the gravitational effects of the nonhomogeneous fluid column. To study its stability, we first note the finite gain stability of $\tilde{k}(s)$ and then conclude using the small again theorem.

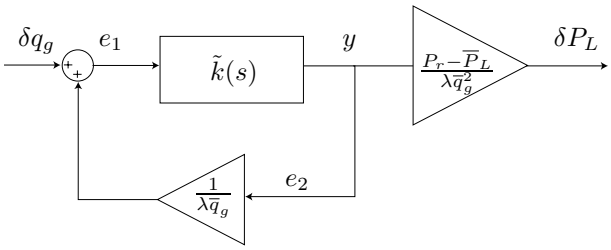

Fig. 5. Block scheme of the tubing subsystem linearized around an equilibrium point. Gravitational effects of the nonhomogeneous fluid column take the form of an inner positive feedback loop.

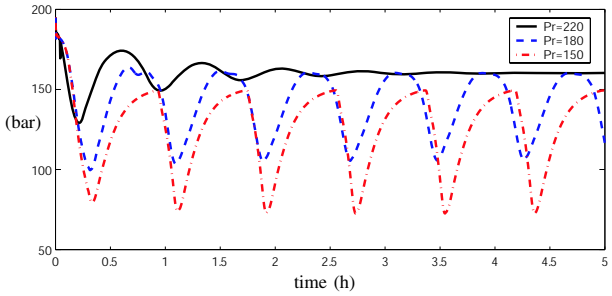

Fig. 6. Simulation in OLGA®2000 of the impact of the pressure reservoir on the stability of the well.

In the following, we denote $\|\cdot\|$ any $\mathcal{L}_p$ norm.

Proposition 1. *With the notations given in Figure 5, there exists a positive constant γ_k such that*

$$\|y\| \leq \gamma_k \|e_1\| \tag{21}$$

Proof: We compute

$$\|k\|_{\mathcal{L}_1} = \frac{|k_1|\tau^2}{2} + |k_2|\tau < +\infty$$

Denoting $\gamma_k = \|k\|_{\mathcal{L}_1}$ and referring to [7][Lemma A.6.5] we directly derive equation (21). ■

Proposition 2. *With the notations given in Figure 5, there exists a positive constant $\overline{q}_g^{min}$ and $\gamma' : [\overline{q}_g^{min}, +\infty[\ni \overline{q}_g \mapsto \mathbb{R}^+\backslash\{0\}$, bounded and continuous, such that*

$$\|\delta P_L\| \leq \gamma'(\overline{q}_g)\|\delta q_g\| \tag{22}$$

Moreover, $\lim_{+\infty} \gamma' = 0$.

Proof: Recalling notations given in Figure 5, we get

$$e_1(t) = \delta q_g(t) + \frac{1}{\lambda \overline{q}_g} y(t)$$

Proposition 1 yields

$$\|e_1\| \leq \|\delta q_g\| + \frac{1}{\lambda \overline{q}_g}\gamma_k \|e_1\| \tag{23}$$

Define $\overline{q}_g^{min} > \frac{\gamma_k}{\lambda}$. For all $\overline{q}_g > \overline{q}_g^{min}$, we can write $\|e_1\| \leq \frac{1}{1-\frac{\gamma_k}{\lambda \overline{q}_g}}\|\delta q_g\|$ and thus,

$$\|P_L\| \leq \frac{P_r - \overline{P}_L}{\lambda \overline{q}_g^2} \frac{\gamma_k}{1-\frac{\gamma_k}{\lambda \overline{q}_g}} \|\delta q_g\|$$

Finally, replacing $\overline{P}_L$ by its expression (17) and noting that $\gamma_k = -\int_0^\tau k(\zeta)d\zeta$ gives

$$\|P_L\| \leq \left(\int_0^\tau -\lambda k\right) \frac{P_r - P_L^\star - \int_0^\tau k}{\left(\lambda \overline{q}_g\right)^2 - \left(\int_0^\tau k\right)^2} \|\delta q_g\|$$

Therefore, we get the desired result with

$$\gamma'(\overline{q}_g) = \left(\int_0^\tau -\lambda k\right) \frac{P_r - P_L^\star - \int_0^\tau k}{\left(\lambda \overline{q}_g\right)^2 - \left(\int_0^\tau k\right)^2} \tag{24}$$

And $\lim_{+\infty} \gamma' = 0$. ■

5) Conclusion and discussion on stability of the tubing: Clearly, the preceding derivation follows along the lines of the proof of the small-gain theorem (as exposed in [15]). If two systems are finite-gain stable and if the product of their gain is small enough (smaller than 1) the system resulting from their connection is also finite gain stable. Recalling that γ_k derives from the integration of Equation (10), here, the condition that guarantees stability is

$$\frac{\gamma_k}{\lambda \overline{q}_g} = \frac{Lg}{RT\lambda \overline{q}_g}\left(RT\rho_l - \frac{1}{2}(P_r + P_0)\right) < 1 \tag{25}$$

From this, we can analyze the impact of several parameters on the behavior of the subsystem.

Increasing $\overline{q}_g$ will tend to lower the gain. Therefore, there exists a lower bound on gas injection rate that guarantees stability. This is consistent with the experimental conclusions found in [12]. These are based on OLGA2000® simulations. In the same study, it also appears that an increase of reservoir pressure leads to more stability. Again, from equation (25), we conclude to the same result. We report in Figure 6, tests done with values for P_r ranging from 150 to 220 bar. Some of the corresponding well parameters are gathered in Table I, under the sign $^{(2)}$. At $Pr = 220$ bar, the system is eventually stable. We note that it is a marginal effect compared to an increase of the gas injection rate. This analysis provides some insights for middle to long-term aging phenomenon of reservoirs when pressure tends to decrease with time.

Further studies reveal that a decrease of ρ_l or L provides more stability. On the other hand, an increase of λ achieved through a decrease of PI tends to improve stability. These parameters are known for their stabilizing effects and can be taken into account at the design stage, e.g. to forecast instability issues.

We notice that the well-known fact that choking has a stabilizing effect is once again verified (see [12]): by increasing P_0 we can let the gain in (25) be smaller than 1. This is one of the key idea behind the FCW controller. In fact, choking can be used in open loop or closed loop to reach unstable points (see [19]).

Quite surprisingly, parameters such as velocity and tubing diameter do not appear in equation (25). This is due to our simplifying assumptions. In fact, both impact on stability through the definition of flow regimes, e.g. bubbly or slug

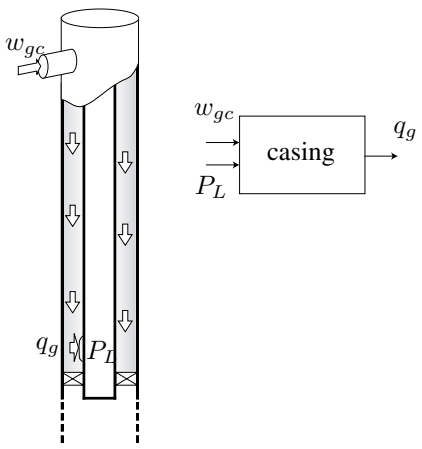

(a) Outline (b) Block scheme

Fig. 7. (a) Outline of the casing. (b) The inputs of the system are the gas mass injection rate w_{gc} and the boundary condition P_L (the downhole pressure). The output is the gas rate entering the tubing: q_g.

flow (see [5]). We have restricted our study to a single slip velocity law. Our model does not represent changes in flow regime and thus does not address hydrodynamic slug instability (see [5]). This could be a direction of future work.

Moreover, using the small gain theorem is a conservative approach. It does not provide an exact value for the turning point from stability to instability. A closer study of the location of the roots of the characteristic equation underlying (18) is needed. Such a study is performed in [20], dealing with the impact of the gas injection rate and quantitatively showing that below a computable limit the roots are located in the left half plane.

III. Stability analysis with a connected casing

Casing and tubing, presented in Figure 1 are connected according to the scheme in Figure 10. While each of these blocks can independently be stable, the resulting connected system may be unstable. Therefore, even under the formal assumption that guarantees the absence of density-wave instability, casing-heading can still occur. A prime example is the casing-heading phenomenon simulated in Figure 8 by adding a casing to the stable case ($P_r = 220$ bar) of Figure 6. Again, feedback connection plays a key role. Following [13], we use a simple first order model for the casing and perform an analysis. Among several conclusions, it appears that large amounts of gas prevent casing-heading instability.

A. Casing-heading instability description

A casing can be considered as an annular buffer filled with gas from a gas network (see Figure 7). Nomenclature is given in I.

Figure 8 shows an example of the casing-heading phenomenon. This cycle consists of three main phases.

1) The upstream pressure is smaller than P_L, therefore no gas enters the tubing. The annulus pressure builds up until it reaches P_L. The gas injection in the tubing begins.
2) As gas mixes with oil in the tubing, the column lightens and the well starts producing. The gas injection rate does not fulfil the well's need. Therefore the pressure in the casing drops. Production reaches a maximum.
3) Annulus pressure drops carrying along the injection gas rate q_g and the oil production. Less gas being injected, the oil column gets heavier and P_L exceed the upstream pressure. Gas injection in the tubing stops.

The OLGA®2000 setup, which is given in Figure 9, is almost the same as in the density-wave case-study presented in Section II-A.1. Main changes are the replacement of the `BUFFER` branch by a 2400 m long vertical pipe: the casing and the boundary condition at the gas inlet which is now defined as a flow condition. One can check the close matching with results presented in [11]. Some of the constants used to simulate the casing-heading phenomenon are referenced in table I under the sign $^{(3)}$.

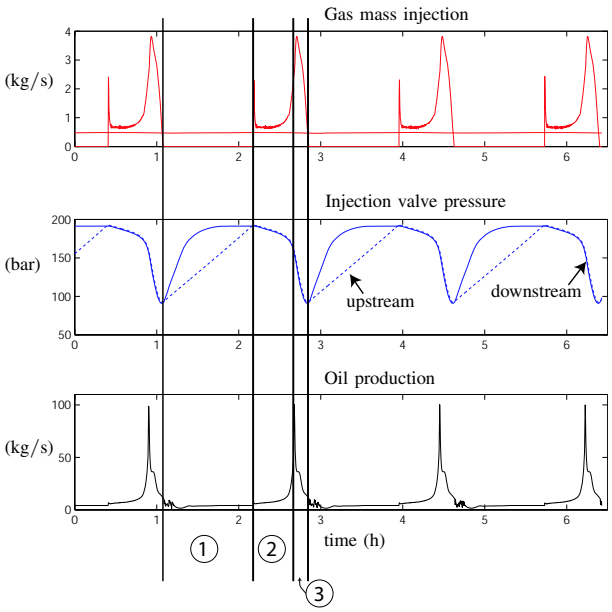

Fig. 8. Casing-heading phenomenon simulated with OLGA®2000.

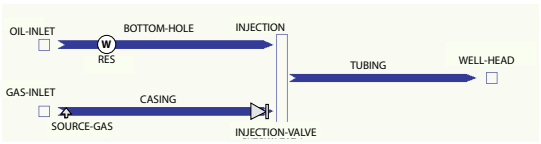

Fig. 9. Block scheme of the OLGA®2000 simulation setup for the casing-heading study phenomenon. It is almost the same as for the density-wave, but the constant gas flow rate is injected before the compressible gas volume. The `injection-valve` is not flow controlled anymore.

B. Casing model

Assuming that the gas is ideal and that the column is at equilibrium, we get

$$\rho_a \triangleq \alpha m_1 \text{ and } p_a \triangleq \beta m_1 \tag{26}$$

where α, β are defined by

$$\alpha RT = \frac{g}{S_a}\frac{1}{1-\exp\left(-\frac{gL_a}{RT}\right)} = \beta \tag{27}$$

We consider as model the mass balance equation in the annulus volume

$$\begin{cases} \dot{m}_1 = w_{gc} - q_g(m_1, P_L) \\ q_g(m_1, P_L) = C_{iv}\sqrt{\alpha m_1 \max(\beta m_1 - P_L, 0)} \end{cases} \tag{28}$$

Stability analysis and equilibrium point definition: We assume normal flowing conditions, i.e. the pressure in the casing is sufficient to counteract $\overline{P}_L$ and to let the gas flow out. Given constant input values $\overline{w}_{gc}$ and $\overline{P}_L$, the equilibrium point is

$$\overline{m}_1 = \frac{1}{\beta}\left(\overline{P}_L + \sqrt{\overline{P}_L^2 + 4\frac{\overline{w}_{gc}^2}{\alpha\beta C_{iv}^2}}\right) \tag{29}$$

Linearization of equation (28) yields, for constant input w_{gc},

$$\begin{cases} \delta\dot{m}_1 = -\dfrac{\partial q_g}{\partial m_1}(\overline{w}_{gc}, \overline{P}_L)\delta m_1 - \dfrac{\partial q_g}{\partial P_L}(\overline{w}_{gc}, \overline{P}_L)\delta P_L \\ \delta q_g = \dfrac{\partial q_g}{\partial m_1}(\overline{w}_{gc}, \overline{P}_L)\delta m_1 + \dfrac{\partial q_g}{\partial P_L}(\overline{w}_{gc}, \overline{P}_L)\delta P_L \end{cases} \tag{30}$$

with

$$\frac{\partial q_g}{\partial m_1}(\overline{w}_{gc}, \overline{P}_L) = \frac{C_{iv}^2\alpha}{2\overline{w}_{gc}}\sqrt{\overline{P}_L^2 + \frac{4\beta}{\alpha}\frac{\overline{w}_{gc}^2}{C_{iv}^2}} \tag{31}$$

$$\frac{\partial q_g}{\partial P_L}(\overline{w}_{gc}, \overline{P}_L) = -\frac{C_{iv}^2\alpha}{4\beta\overline{w}_{gc}}\left(\overline{P}_L + \sqrt{\overline{P}_L^2 + \frac{4\beta}{\alpha}\frac{\overline{w}_{gc}^2}{C_{iv}^2}}\right) \tag{32}$$

Proposition 3. *For $\overline{w}_{gc} > 0$ the equilibrium point of* (30) *is exponentially stable. Therefore, the linearized system* (30) *is finite gain stable. One can find $(\gamma, \mu) : (\mathbb{R}\backslash\{0\})^2 \mapsto (\mathbb{R}^+\backslash\{0\})^2$, bounded and continuous, such that*

$$\|\delta q_g\| \leq \gamma(\overline{w}_{gc}, \overline{P}_L)\|P_L\| + \mu(\overline{w}_{gc}, \overline{P}_L) \tag{33}$$

These functions are

$$\gamma = \frac{C_{iv}^2\alpha}{2\overline{w}_{gc}}\sqrt{\overline{P}_L^2 + \frac{4\beta}{\alpha}\frac{\overline{w}_{gc}^2}{C_{iv}^2}} \tag{34}$$

$$\mu = m_1(0)\sqrt{\frac{C_{iv}^2\alpha}{8\beta\overline{w}_{gc}}\left(\overline{P}_L + \sqrt{\overline{P}_L^2 + \frac{4\beta}{\alpha}\frac{\overline{w}_{gc}^2}{C_{iv}^2}}\right)} \tag{35}$$

Proof: By assumption, the equilibrium point is such that $\overline{w}_{gc} > 0$, then

$$-\frac{\partial q_g}{\partial m_1}(\overline{w}_{gc}, \overline{P}_L) < 0$$

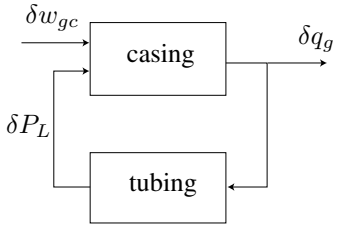

Fig. 10. Block scheme of the interconnected systems linearized around an equilibrium point.

Using explicit formulas given in [15][Corollary 5.2] for linear systems, we can write (33) with

$$\gamma(\overline{w}_{gc}, \overline{q}_g) = 2\left|\frac{\partial q_g}{\partial P_L}(\overline{w}_{gc}, \overline{P}_L)\right|$$

$$\mu(\overline{w}_{gc}, \overline{q}_g) = \frac{1}{\sqrt{2}}m_1(0)\sqrt{\frac{\partial q_g}{\partial m_1}(\overline{w}_{gc}, \overline{P}_L)}$$

which concludes the proof. ∎

C. Stability analysis of the connected system

1) Stability criterion: We now consider the connected linearized system defined by

$$\begin{cases} \delta\dot{m}_1 = -\dfrac{\partial q_g}{\partial m_1}(\overline{w}_{gc}, \overline{P}_L)\delta m_1 - \dfrac{\partial q_g}{\partial P_L}(\overline{w}_{gc}, \overline{P}_L)\delta P_L \\ \delta q_g = \dfrac{\partial q_g}{\partial m_1}(\overline{w}_{gc}, \overline{P}_L)\delta m_1 + \dfrac{\partial q_g}{\partial P_L}(\overline{w}_{gc}, \overline{P}_L)\delta P_L \\ \delta P_L(t) = \displaystyle\int_0^\tau k(\zeta)\frac{1}{\lambda\overline{q}_g}\delta P_L(t-\zeta)d\zeta \\ \qquad + \displaystyle\int_0^\tau k(\zeta)\frac{P_r - \overline{P}_L}{\lambda q_g^2}\delta q_g(t-\zeta)d\zeta \end{cases} \tag{36}$$

In Proposition 2 and 3 respectively, we derived the gain of the tubing and casing subsystems. Gathering and connecting these requires to match their equilibrium points. This defines a constraint on $\overline{P}_L$ and $\overline{q}_g$. For $\overline{w}_{gc} > 0$, equilibria are defined by (37). New expressions for gains through the connections are given in (38), (39) and (40).

$$\begin{cases} \overline{q}_g = \overline{w}_{gc} \\ \overline{P}_L = \dfrac{\lambda\overline{w}_{gc}\left(P_L^\star + \int_0^\tau k(\zeta)d\zeta\right) - P_r\int_0^\tau k(\zeta)d\zeta}{\lambda\overline{w}_{gc} - \int_0^\tau k(\zeta)d\zeta} \end{cases} \tag{37}$$

$$\hat{\gamma}(\overline{w}_{gc}) = \gamma(\overline{w}_{gc}, \overline{P}_L) \tag{38}$$

$$\hat{\mu}(\overline{w}_{gc}) = \mu(\overline{w}_{gc}, \overline{P}_L) \tag{39}$$

$$\hat{\gamma}'(\overline{w}_{gc}) = \gamma'(\overline{q}_g) \tag{40}$$

Proposition 4. *There exists a positive constant $\overline{w}_{gc}^{min}$ such that for all $\overline{w}_{gc} > \overline{w}_{gc}^{min}$ system* (36) *is finite-gain stable.*

Proof: From equations (22), (33) and (38), (39) and (40) we get

$$\|\delta q_g\| \leq \hat{\gamma}(\overline{w}_{gc})\|\delta P_L\| + \hat{\mu}(\overline{w}_{gc})$$
$$\|\delta P_L\| \leq \hat{\gamma}'(\overline{w}_{gc})\|\delta q_g\|$$

Notice that $\lim_{+\infty} \hat{\gamma}' = 0$ and $\lim_{+\infty} \hat{\gamma} > 0$. Therefore, there exists $\overline{w}_{gc}^{min}$ such that for all $\overline{w}_{gc} > \overline{w}_{gc}^{min}$

$$\hat{\gamma}(\overline{w}_{gc})\hat{\gamma}'(\overline{w}_{gc}) < 1 \tag{41}$$

The small gain theorem implies that the connected system (36) is finite gain stable. ■

Using the fact that

$$\int_0^\tau k(\zeta)d\zeta = Lg\left(\frac{P_0 + P_r}{2RT} - \rho_l\right) \tag{42}$$

We compute

$$\overline{P}_L = \frac{\lambda\overline{w}_{gc}\left(P_0 + Lg\frac{P_0+P_r}{2RT}\right) - P_r Lg\left(\frac{P_0+P_r}{2RT} - \rho_l\right)}{\lambda\overline{w}_{gc} - Lg\left(\frac{P_0+P_r}{2RT} - \rho_l\right)} \tag{43}$$

Therefore,

$$\hat{\gamma}' = \left(\frac{P_0 + P_r}{2RT} - \rho_l\right)\frac{\lambda Lg(P_0 - P_r + Lg\frac{P_0+P_r}{2RT})}{(\lambda\overline{w}_{gc})^2 - (Lg)^2\left(\frac{P_0+P_r}{2RT} - \rho_l\right)^2} \tag{44}$$

and

$$\hat{\gamma}(\overline{w}_{gc}) = \frac{C_{iv}^2\alpha}{2\overline{w}_{gc}}\sqrt{\overline{P}_L^2 + \frac{4\beta}{\alpha}\frac{\overline{w}_{gc}^2}{C_{iv}^2}} \tag{45}$$

2) Conclusion and discussion: From equations (41), (44) and (45), we can analyze the influence of several parameters on the interconnected system. The best known effect is the role of the C_{iv} parameter. As reported in [12], it is necessary for stability to maintain the flow through the injection valve critical. This is guaranteed by a choice of a small diameter injection valve, which corresponds in our model to a small C_{iv}. Indeed, reducing C_{iv} lowers $\hat{\gamma}$ in equation (45), and thus ultimately guarantees inequality (41) and provides stability. Other important parameters are α and β (defined in equation (26)) through which S_a, the section of the casing, plays a key role. Increasing S_a decreases α and β. Eventually, $\hat{\gamma}$ provides stability through inequality (41). In physical terms, the stabilizing buffer effect is emphasized by increasing the volume, therefore a bigger section lowers the coupling effect.

IV. Conclusion and future work

At two levels of modelling, we underline the role of inner feedback loops on stability. Many well-known effects can be interpreted in terms of variations of these two loops gains. This is particularly true for the gas rate, the reservoir pressure and the flow rate coefficient as shown in Sections II-B.5 and III-C.2. Numerical simulations confirm this analysis. This work can be made more general, through a wide simulation test campaign. Following [10], stability maps could be established. For example, it would be interesting to determine injection requirements with respect to a specification of reservoir pressure values. Among many applications, this could serve as a conservative bound in the gas allocation problem of a network of heterogeneous oil wells within an oil field [16]. Establishing these stability maps is a future direction of our work.

References

[1] F. J. S. Alhanati, Z. Schmidt, D. R. Doty, and D. D. Lageref, "Continuous gas-lift instability: diagnosis, criteria, and solutions," in *68th Annual Technical Conference and Exhibition*, no. SPE 26554, Houston, TX, October 1993.

[2] H. Asheim, "Criteria for gas-lift stability," *Journal of Petroleum Technology*, pp. 1452–1456, 1988.

[3] E. P. Blick, P. N. Enga, and P. C. Lin, "Theoretical stability analysis of flowing oil wells and gas-lift wells," *SPEPE*, pp. 508–514, 1988.

[4] K. E. Brown, *Gas lift theory and practice*. Petroleum publishing CO., Tulsa, Oklahoma, 1973.

[5] H. Cholet, *Well production. Practical handbook*. Editions TECHNIP, 2000.

[6] A. J. Chorin and J. E. Marsden, *A mathematical introduction to fluid mechanics*. Springer-Verlag, 1990.

[7] R. F. Curtain and H. J. Zwart, *An introduction to infinite-dimensional linear systems theory*, ser. Text in Applied Mathematics, 21. Springer-Verlag, 1995.

[8] E. E. DeMoss and W. D. Tiemann, "Gas lift increases high-volume production from Claymore field," *Journal of Petroleum Technology*, no. SPE 9214, pp. 696–702, 1982.

[9] E. Duret, "Dynamique et contrôle des écoulements polyphasiques," Ph.D. dissertation, École des Mines de Paris, 2005.

[10] Y. V. Fairuzov, I. Guerrero-Sarabia, C. Calva-Morales, R. Carmona-Diaz, and T. C.-B. ans N. Miguel-Hernandez ans A. Rojas-Figueroa, "Stability maps for continuous gas-lift wells: new approach to solving an old problem," in *SPE Annual Technical Conference and Exhibition*, no. SPE 90644, 2004.

[11] A. W. Grupping, C. W. F. Lucas, and F. D. Vermeulen, "Continuous-flow gas-lift. These methods can eliminate or control annulus headings," *Oil and Gas Journal*, pp. 186–192, 1984.

[12] B. Hu and M. Golan, "Gas-lift instability resulted production loss and its remedy by feedback control: dynamical simulation results," in *SPE International Improved Oil Recovery Conference in Asia Pacific*, no. SPE 84917, Kuala Lumpur, Malaysia, 2003.

[13] L. S. Imsland, "Topics in nonlinear control - ouput feedback stabilization and control of positive systems," Ph.D. dissertation, Norwegian University of Science and Technology, Department of Engineering and Cybernetics, 2002.

[14] B. Jansen, M. Dalsmo, K. Havre, L. Nøkleberg, V. Kritiansen, and P. Lemétayer, "Automatic control of unstable gas-lifted wells," *SPE Annual technical Confererence and Exhibition.*, no. SPE 56832, October 1999.

[15] H. K. Khalil, *Nonlinear Systems*. MacMillan, 1992.

[16] K. K. Lo, "Optimum lift-gas allocations under multiple production constraints," 1992.

[17] Scandpower, *OLGA® 2000 User's Manual*. Scandpower, 2004.

[18] L. Sinègre, N. Petit, P. Lemétayer, P. Gervaud, and P. Ménégatti, "Casing heading phenomenon in gas lifted well as a limit cycle of a 2d model with switches," in *Proc. of the* 16*th IFAC World Congress*, 2005.

[19] ——, "Contrôle des puits activés en gas-lift," in *10th Congress of Société Française du Génie des Procédés*, 2005.

[20] L. Sinègre, N. Petit, and P. Ménégatti, "Distributed delay model for density wave dynamics in gas lifted wells," in *Proc. of the* 44*th IEEE Conf. on Decision and Control*, 2005.

[21] A. J. Torre, Z. Schmidt, R. N. Blais, D. R. Doty, and J. P. Brill, "Casing heading in flowing wells," *SPE Production Engineering*, no. SPE 13801, 1987.

[22] Z. G. Xu and M. Golan, "Criteria for operation stability of gas lift," *SPE paper*, no. 19362, 1989.